

This is a self-archived version of an original article. This version may differ from the original in pagination and typographic details.

Author(s): Bonnard, J.; Dobaczewski, J.; Danneaux, G.; Kortelainen, M.

Title: Nuclear DFT electromagnetic moments in heavy deformed open-shell odd nuclei

Year: 2023

Version: Published version

Copyright: © 2023 The Author(s). Published by Elsevier B.V. Funded by SCOAP3.

Rights: CC BY 4.0

Rights url: <https://creativecommons.org/licenses/by/4.0/>

Please cite the original version:

Bonnard, J., Dobaczewski, J., Danneaux, G., & Kortelainen, M. (2023). Nuclear DFT electromagnetic moments in heavy deformed open-shell odd nuclei. *Physics Letters B*, 843, Article 138014. <https://doi.org/10.1016/j.physletb.2023.138014>



Nuclear DFT electromagnetic moments in heavy deformed open-shell odd nuclei

J. Bonnard^{a,b}, J. Dobaczewski^{a,c,*}, G. Danneaux^d, M. Kortelainen^d

^a School of Physics, Engineering and Technology, University of York, Heslington, York YO10 5DD, United Kingdom

^b Université de Lyon, Institut de Physique des 2 Infinis de Lyon, IN2P3-CNRS-UCBL, 4 rue Enrico Fermi, 69622 Villeurbanne, France

^c Institute of Theoretical Physics, Faculty of Physics, University of Warsaw, ul. Pasteura 5, PL-02-093 Warsaw, Poland

^d Department of Physics, University of Jyväskylä, PB 35(YFL), FIN-40014 Jyväskylä, Finland

ARTICLE INFO

Article history:

Received 9 May 2023

Received in revised form 2 June 2023

Accepted 8 June 2023

Available online 13 June 2023

Editor: A. Schwenk

Dataset link: [Version \(v3.16n\) of code hfodd that was used in this study along with the corresponding raw input and output data files \(Original Data\)](#)

Keywords:

Mean field

Electromagnetic moments

Symmetry restoration

ABSTRACT

Within the nuclear DFT approach, we determined the magnetic dipole and electric quadrupole moments for paired nuclear states corresponding to the proton (neutron) quasiparticles blocked in the $\pi 11/2^-$ ($\nu 13/2^+$) intruder configurations. We performed calculations for all deformed open-shell odd nuclei with $63 \leq Z \leq 82$ and $82 \leq N \leq 126$. Time-reversal symmetry was broken in the intrinsic reference frame and self-consistent shape and spin core polarizations were established. We determined spectroscopic moments of angular-momentum-projected wave functions and compared them with available experimental data. We obtained good agreement with data without using effective g-factors or effective charges in the dipole or quadrupole operators, respectively. We also showed that the intrinsic magnetic dipole moments, or those obtained for conserved intrinsic time-reversal symmetry, do not represent viable approximations of the spectroscopic ones.

© 2023 The Author(s). Published by Elsevier B.V. This is an open access article under the CC BY license (<http://creativecommons.org/licenses/by/4.0/>). Funded by SCOAP³.

Electromagnetic moments offer a wealth of information for understanding structure of atomic nuclei. Indeed, while electric quadrupole moments shed light on shapes of nuclei, and thus probe the collective degrees of freedom, magnetic dipole moments are more closely related to single-particle aspects such as shell properties of valence nucleons [1,2]. Over the time, considerable efforts have been undertaken by experimentalists to develop new techniques allowing us to access electromagnetic moments of more and more exotic isotopes [3]. Experimental trends in many isotopic chains have now been measured, for ground states as well as excited and isomeric states, see for example recent work in Ref. [4].

In this Letter, we present the results of the first systematic mean-field calculations of spectroscopic electromagnetic moments in heavy deformed open-shell paired odd nuclei, which offers the methodology to interpret measurements performed within thousands of experiments. We focus on the $11/2^-$ and $13/2^+$ isomeric and ground states of nuclei with proton and neutron numbers of $63 \leq Z \leq 82$ and $82 \leq N \leq 126$, for which a significant amount of data is now available [5–8]. In Fig. 1, we show an overview of the

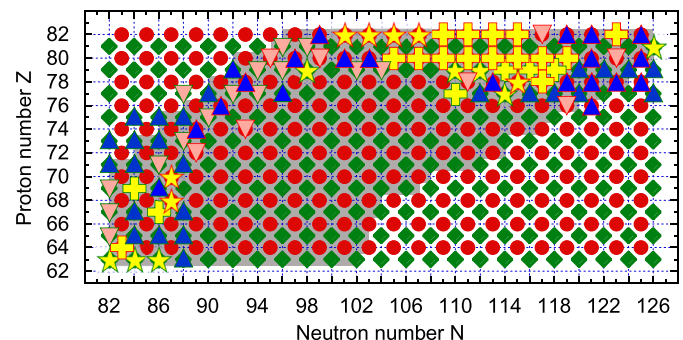


Fig. 1. Schematic illustration of the set of the odd- Z (diamonds) and odd- N (circles) nuclei investigated in this work. Stars (plus signs) represent nuclei where only magnetic dipole moments (magnetic dipole and electric quadrupole moments) have so far been measured [5–8]. Up triangles (down triangles) represent nuclei where the $11/2^-$ or $13/2^+$ states were experimentally identified (tentatively identified) [9]. Shaded area illustrates the region of nuclei with known masses [10].

considered region of the Segré chart and indicate nuclei where different types of experimental data are known.

It appears that no theoretical model of nuclear structure is able to provide a satisfying unified and global description of electro-

* Corresponding author.

E-mail address: jacek.dobaczewski@york.ac.uk (J. Dobaczewski).

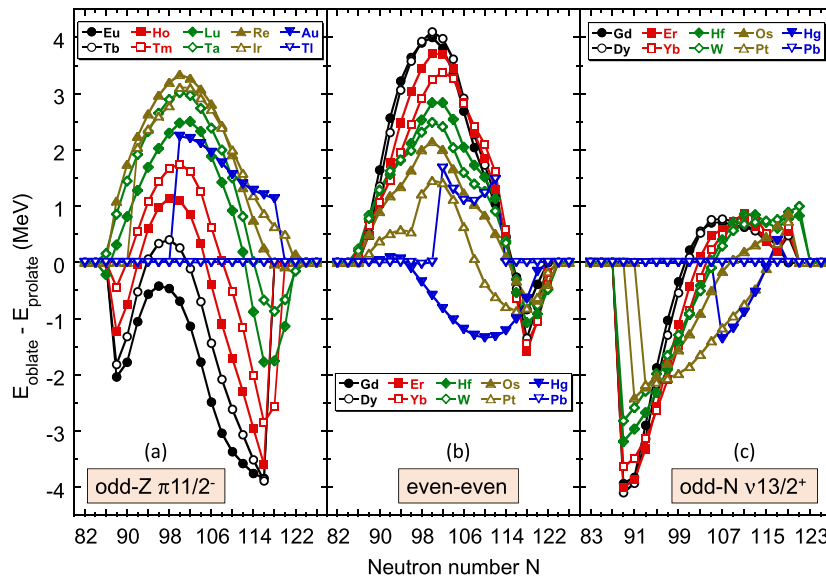


Fig. 2. Differences of energies at oblate and prolate minima calculated for the odd- $Z \pi 11/2^-$ configurations (a), even-even nuclei (b), and odd- $N \nu 13/2^+$ configurations (c). Lines reverting to the values of $E_{\text{oblate}} - E_{\text{prolate}} = 0$ denote cases where either oblate or prolate higher-energy minimum disappears.

magnetic moments. On the one hand, great progress was achieved by *ab initio* approaches for light species [11], but their extension to heavier systems remains challenging because of the necessity to include extensive many-body correlations [12], many-body currents [13], or unmanageably large phase spaces [14]. On the other hand, traditional shell-model successfully describes experimental electromagnetic moments [3,15–17]. Nonetheless, such calculations often resort to effective g -factors or effective charges tuned to reproduce specific data in limited regions of the chart of nuclei, so much so that the values obtained in different regions are not consistent. Finally, nuclear density-functional theory (DFT) has proved to perform globally well for charge radii and electric quadrupole moments of even-even nuclei across the nuclear chart [18,19]. In contrast, however, DFT calculations in open-shell odd systems still demand further developments to allow for an overall good description of electromagnetic moments [20–27].

This Letter presents the results of the first systematic calculation of the spectroscopic magnetic dipole and electric quadrupole moments that go beyond current state-of-the-art. In a recent publication [28], we have laid out the basics of our DFT approach and applied it to selected nuclei without pairing correlations. Here, by including pairing, we port the method's applicability to all nuclei. This constitutes a major advancement in the field because, apart from formulating general principles of symmetry restoration for blocked states [29,30] and a few applications in selected odd nuclei [20,27], no systematic implementation thereof in heavy odd nuclei existed so far. Nevertheless, we also note that Refs. [20,27] go beyond our study by including triaxial shapes and generator-coordinate-method collective correlations.

In addition, we bring about an important new strategy by performing analyses for specific fixed configurations, irrespective of their detailed excitation energies above the ground states. This allows us to follow selected configurations across many nuclei, in function of numbers of protons or neutrons, and thus to gain better physical insight into the properties of these configurations. To follow specific configurations, we implemented the following four-step procedure.

First, we performed a simple unpaired calculation of a doubly magic spherical nucleus ^{208}Pb . In the second step, by breaking spherical and time-reversal symmetries and using weak constraints on axial intrinsic quadrupole moment Q_{20} and angular-momentum projection I_z [31], we determined weakly prolate and

oblate ^{208}Pb states with the axial symmetry axis and single-particle angular momenta aligned along the z -axis. At this point, we could identify the required single-particle wave functions of states originating from the spherical proton $h_{11/2}$ and neutron $i_{13/2}$ orbitals that have good values of parity π and projection Ω on the axial-symmetry axis of $\Omega^\pi = +11/2^-$ and $\Omega^\pi = +13/2^+$, respectively. These two selected single-particle states were then fixed and used to tag quasiparticle states [32,33] in the quasiparticle-blocking calculations required for the paired odd- Z and odd- N axial nuclei considered here.

In the third step, we performed tagged quasiparticle-blocking calculations by fixing the average constant neutron and proton pairing gaps [34] at $\Delta_n = \Delta_p = 1$ MeV and constraining the intrinsic mass quadrupole moments to either $Q_{20} = -10$ or $+10$ b. This allowed us to determine stable starting-point solutions that, in the fourth-step, were reconverged to the self-consistent oblate or prolate minima, respectively, by relaxing the constraints on the quadrupole moments and replacing the fixed pairing gaps by pairing forces. In addition, next to the closed shells, that is, for $N = 82, 83, 125$, and 126 or $Z = 81$ and 82 , where the neutron or proton pairing correlations disappear, we performed calculations with the paired solutions explicitly switched over to the unpaired ones [35]. To follow the same configurations as those tagged in the quasiparticle-blocking paired solutions, in version (v3.16n) of code HFODD [36], we implemented the tagging technique also for unpaired states [37].

As it turned out, for the majority of the studied nuclei, both oblate and prolate minima were obtained. However, as shown in Fig. 2, the oblate-prolate energy differences obtained in the odd- Z and odd- N nuclei were very different from one another, and also both were very different from those in neighboring even-even nuclei. It appears that without a fully self-consistent calculation, in an open-shell nucleus one cannot *a priori* guess how an odd particle would polarize the even system.

Finally, we determined the standard spectroscopic moments [38] by performing the angular-momentum projection (AMP) [39] of the obtained intrinsic paired and unpaired states. This was done using version (v3.16n) of code HFODD [35,36], with the Pfaffian method used to determine overlaps of blocked paired states [29,40]. We also tested the effects of the particle-number projection (PNP) [35,39], performed together with the AMP. This turned out to give the magnetic dipole and electric quadrupole

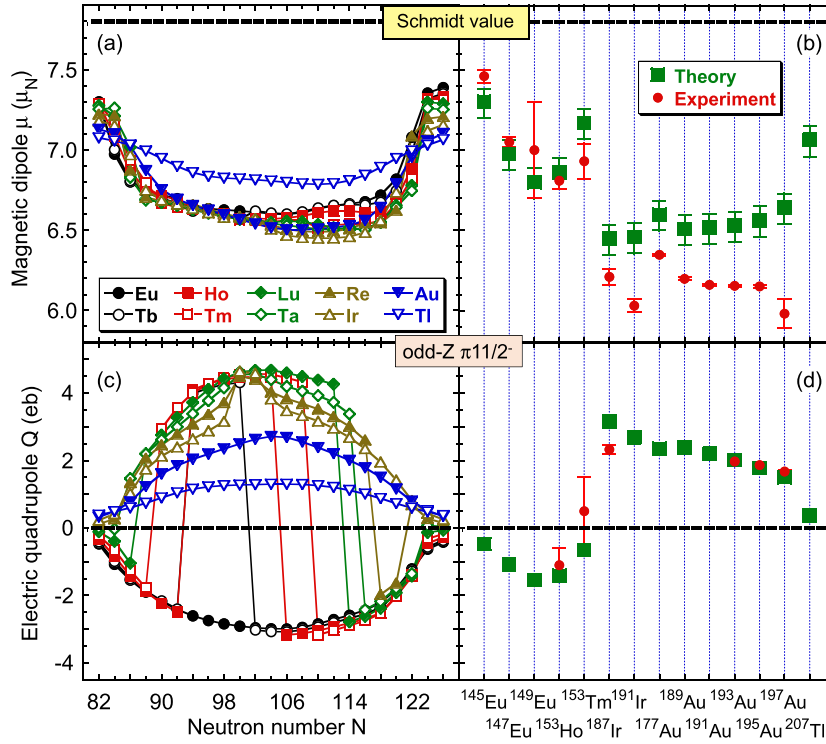


Fig. 3. Calculated magnetic dipole μ (a) and electric quadrupole Q (c) moments of the $\pi 11/2^-$ configurations in odd- Z nuclei compared in panels (b) and (d) with the available experimental data [5–8]. Theoretical error bars correspond to the uncertainty of the isovector Landau parameter $g'_0 = 1.7(4)$, see details presented in Refs. [28,41].

moments within about 1% of the AMP-only values [41]. Therefore, the AMP+PNP calculations, which take about two orders of magnitude more CPU time than those performed for the AMP-only, can be safely avoided.

In this Letter, we considered the Skyrme functional UNEDF1 [42] with the pairing correlations treated within the standard two-basis method [43,44] for the single-particle states cut at 60 MeV. The neutron and proton pairing strengths were increased by 20% with respect to the original UNEDF1 parameter adjustment. Tests have shown that such an increase compensates for the effects of the Lipkin-Nogami approximate PNP [39], which was not used in this work. An essential element of our approach is the mean-field time-reversal-symmetry breaking induced by the spin-spin interaction implemented in terms of the isovector Landau parameter g'_0 . We used the value of $g'_0 = 1.7(4)$ adjusted in Ref. [28], see also the Supplemental Material [41], and there were no other parameters adjusted in the present work.

Figs. 3 and 4 summarize principal results of our study obtained for the $\pi 11/2^-$ configurations in odd- Z nuclei and $\nu 13/2^+$ configurations in odd- N nuclei [41]. Across the entire set of nuclei studied here, the corresponding two deformed single-particle states are characterized by the Nilsson labels¹ [505]11/2 and [606]13/2, respectively. Within the studied proton and neutron shell, with increasing numbers of protons or neutrons, the occupation numbers of states [505]11/2 and [606]13/2 are swept between zero and one. This allows us to gain a unique insight into the polarization properties of these two states in the function of the numbers of particles.

The electric quadrupole moments Q , shown in Figs. 3(c) and 4(c), present clear patterns of the particle-number dependence, which has approximately a parabolic shape both on the prolate

and oblate side. Small values of Q obtained near closed shells follow the well-known scheme dictated by the deformation-splitting of spherical orbitals. Indeed, there the high- Ω magnetic substates have the highest (lowest) energies on the prolate (oblate) side, and thus one obtains prolate (oblate) shapes when these orbitals are occupied by holes (particles). What is much less obvious, and what is very clearly born out in our results, is the fact that the same signs of the quadrupole moments are obtained when the configurations are followed away from the closed shells. This has very important consequences, namely, a configuration that begins as a hole (particle) state at the lower end of the particle numbers, somewhere between the magic numbers *must* change the sign of the quadrupole moment. This is so because at the higher end, it terminates as a particle (hole) state. This rule is strictly obeyed in all our results, even if in the middle of the shell the blocked quasi-particles can be below or above the Fermi surface.

Patterns of the particle-number dependence of magnetic dipole moments μ , Figs. 3(a) and 4(a), are different. Near the neutron closed shells, where the quadrupole moments are small, their departures from the single-particle Schmidt limits [45] are dictated by the spin polarizations induced by the time-odd mean fields [28]. Detailed values of these departures can depend relatively strongly ($\pi 11/2^-$ near $N = 126$) or relatively weakly ($\nu 13/2^+$ near $N = 82$) on the numbers of protons in the open shell. With particle numbers moving away from the neutron closed shells, the magnetic dipole moments undergo rather sudden changes and then, in the middle of the shell, their values stabilize. This pattern does not follow the gradual dependence of the quadrupole moments on particle numbers. Moreover, in open-shell nuclei, the magnetic dipole moments appear to be independent of whether the nucleus is oblate or prolate. In addition, for relatively weakly deformed isotopes of Pb and Tl, the dependence of the magnetic dipole moments on the number of neutrons is relatively weak.

Apart from the case of light Hg isotopes, electric quadrupole moments agree with data spectacularly well, Figs. 3(d) and 4(d).

¹ We determined the Nilsson label of a given self-consistent single-particle state by finding the largest amplitude of its expansion onto the deformed axial harmonic-oscillator basis [31].

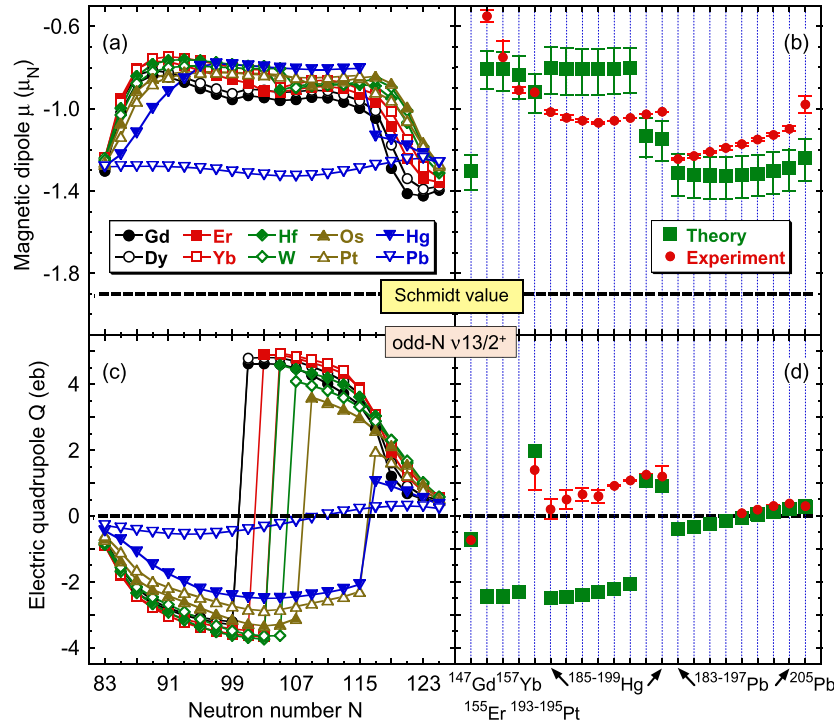


Fig. 4. Same as in Fig. 3 but for the $\nu 13/2^+$ configurations in odd- N nuclei.

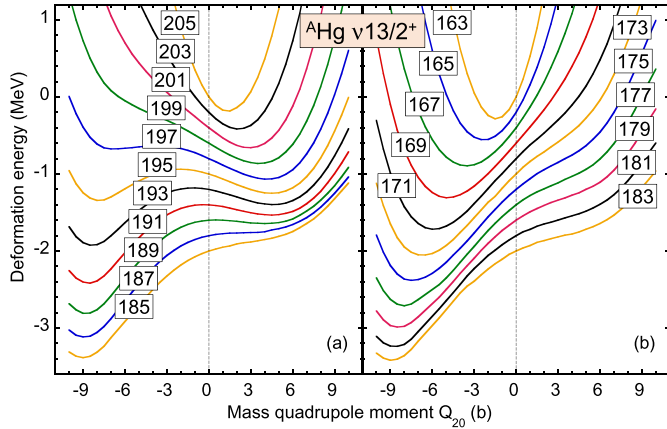


Fig. 5. Deformation energies, $E(Q_{20}) - E(0)$, of the $\nu 13/2^+$ isomers in the Hg isotopes as functions of the intrinsic mass quadrupole moments Q_{20} . For better readability, at $A \geq 185$ (a) and $A \leq 183$ (b), the curves are shifted by $(A - 205) \times 0.1$ MeV and $(163 - A) \times 0.1$ MeV, respectively. Dashed lines mark points at $Q_{20} = 0$.

Also those of the two heaviest measured Hg isotopes are reproduced perfectly. However, in the calculations, lighter Hg isotopes undergo a transition to oblate shapes, which is not born out in the data. As discussed above, such a transition to oblate shapes must occur somewhere in the isotopic chain because the oblate shape is mandated by the particle character of the orbital $\nu 13/2^+$ near $N = 82$. As clearly visible in the results shown in Fig. 2(c) and 5, not only the transition to oblate shapes occurs at $N = 115$, but below $N = 107$, the prolate minimum disappears entirely.

It appears that the same transition to oblate shapes in light Hg isotopes creates a deviation from the smooth trend observed in the measured magnetic dipole moments, Figs. 3(b) and 4(b). Otherwise, the calculated magnetic dipole moments of heavier nuclei seem to call for stronger time-odd polarization effects, whereas

those of lighter nuclei appear to be about right.² Such detailed comparison with data may indicate that more structured interactions in the time-odd mean-field sector should possibly be considered beyond the simple spin-spin interaction employed here.

The magnetic dipole moment of ^{147}Gd is an exception. In this nucleus, the calculated value of $-1.30 \mu_N$ disagrees with the two measured values of $-0.24(7) \mu_N$ [46,47] and $+0.49(2) \mu_N$ [48], which, in addition, are strongly incompatible with one another. A possible mixing of the pure $i_{13/2}$ configuration with the $3^- \otimes f_{7/2}$ contribution was discussed in the literature [48] and in the future work it will also be considered within the present DFT approach. However, such a mixing should neither strongly affect the magnetic dipole moments of neighboring nuclei nor spoil the excellent agreement with the value of the quadrupole moment measured in ^{147}Gd .

We conclude our presentation with a comparison of the spectroscopic and intrinsic magnetic dipole moments determined with and without the time-odd mean fields, Fig. 6. First, we note that without the time-odd mean fields, the calculated intrinsic magnetic dipole moments of all nuclei are exactly equal to the Schmidt limit [45]. This is a simple consequence of the fact that in the intrinsic reference frame, the high-spin intruder configurations studied here have both the orbital and spin angular momenta always maximally aligned along the symmetry axis. This property turns out to be entirely independent of the intrinsic deformation.

With the time-odd mean fields included, the intrinsic magnetic dipole moments move away from the Schmidt limit and become particle-number dependent. However, their values stay entirely uncorrelated with the nuclear deformation. The effect of the deformation only appears when the spectroscopic magnetic dipole moments are evaluated, Fig. 6(a). As can be demonstrated through

² After performing the calculations, we learned that the magnetic dipole moment of ^{207}Tl has already been measured. The obtained experimental value was not published yet.

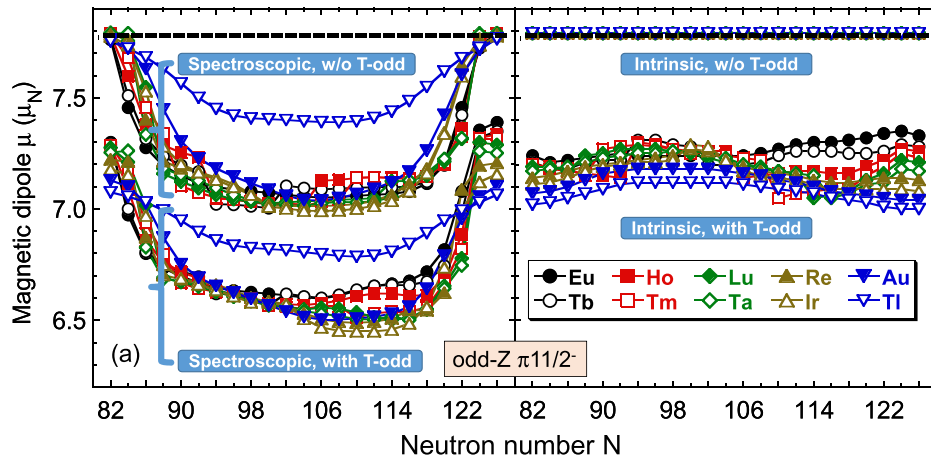


Fig. 6. Spectroscopic (a) and intrinsic (b) magnetic dipole moments calculated for the $\pi 11/2^-$ configurations in odd- Z nuclei with and without the time-odd mean fields.

the particle-core-coupling analysis [4,49], the deformation effects can be traced back to the coupling of the single-particle wave functions with the 2^+ , 4^+ , 6^+ , ... states of the core. These effects turn out to be invisible in the intrinsic reference frame and require the determination of the spectroscopic moments.

The inclusion of the time-odd mean fields breaks the signature symmetry of the core and results in the appearance of the 1^+ , 3^+ , 5^+ , ... states. The coupling of the single-particle wave functions with the core's odd-spin states shifts the magnetic moments away from the Schmidt limit. The magnitude of this shift does not seem to be correlated with the occupations of the spin-orbit partners, which vary within the single-particle shells. This is in contrast to the traditional shell-model interpretation, which is based on the so-called first-order correction to the magnetic moments [2]. In the nuclear DFT, the effects of the time-odd mean fields rather seem to proceed through a democratic (collective) spin polarization of the core.

Since the principal part of the magnetic dipole moment is given by the contribution of the odd particle, the collectivity of the core contribution does not result in a meaningful approximation of the spectroscopic magnetic dipole moment by the intrinsic one. A microscopic evaluation of the spectroscopic magnetic dipole moments is thus mandatory.³ Moreover, the core contribution to the magnetic dipole moment does not seem to be amenable to simple modelization in terms of a smooth function of Z/A , as is the case for the collective rotation, which generates a collective current flow [50]. Altogether, both the angular-momentum symmetry restoration and time-reversal symmetry breaking allowing for inclusion of the time-odd mean fields appear to be essential elements of describing the nuclear magnetic dipole moments.

In conclusion, we presented the results of the first nuclear DFT determination of the magnetic dipole and electric quadrupole moments established in 450 heavy open-shell deformed and paired odd nuclei. We showed that by following fixed single-particle configurations, one could pin down generic properties of the calculated moments and analyze their dependence on the proton and neutron numbers. Apart from pronounced differences that we examined in the Hg isotopes and ^{147}Gd , we obtained good agreement with known experimental data. For that, no effective g -factors or effective charges were needed. We demonstrated an essential role

played by the time-odd core polarization and angular-momentum symmetry restoration. We compared the calculated spectroscopic and intrinsic magnetic dipole moments and showed that the former cannot be meaningfully approximated by the latter.

Our work motivates further experimental and theoretical studies of nuclear electromagnetic moments. In the experiment, depending on the lifetimes of states and availability of beams, moments of many more states $11/2^-$ and $13/2^+$ can probably be measured [8] and compared with our model predictions. This can further inform the nuclear-DFT calculations and allow for needed improvements and extensions to exotic moments. In particular, the role of the coupling between single-particle states and negative-parity core states should be studied and evaluated globally. In addition, multi-reference configuration interaction of different single-particle configurations and/or different K -components related to triaxiality should be analyzed. But first and foremost, calculations pioneered in this work can become the basis of determining electromagnetic moments across the entire Segré chart for all odd nuclei and spins and parities. Work on this extensive goal is now in progress.

Declaration of competing interest

The authors declare that they have no known competing financial interests or personal relationships that could have appeared to influence the work reported in this paper.

Data availability

I have shared the link to my data and code at the Attach File step [Version \(v3.16n\) of code hfodd that was used in this study along with the corresponding raw input and output data files \(Original Data\)](#) (webfiles.york.ac.uk).

Acknowledgements

We thank A.N. Andreyev, A.E. Barzakh, and I.D. Moore for useful discussions. This work was partially supported by the STFC Grant Nos. ST/P003885/1 and ST/V001035/1, by the Polish National Science Centre under Contract No. 2018/31/B/ST2/02220, by a Leverhulme Trust Research Project Grant, and by the Academy of Finland under the Academy Project No. 339243. We acknowledge the CSC-IT Center for Science Ltd., Finland, for the allocation of computational resources. This project was partly undertaken on the Viking Cluster, which is a high performance compute facility provided by the University of York. We are grateful for computational support

³ To a lesser degree, the same observation also holds for the spectroscopic electric quadrupole moments, which, at large deformations, can be precisely approximated by products of the Clebsch-Gordan coefficient squared and intrinsic electric quadrupole moments. This very well known fact is illustrated in the Supplemental Material [41], where we also show that at small deformations, the relative differences can reach 30%.

from the University of York High Performance Computing service, Viking and the Research Computing team.

Appendix A. Supplementary material

Supplementary material related to this article can be found online at <https://doi.org/10.1016/j.physletb.2023.138014>.

References

- [1] H. Kopfermann, E.E. Schneider, *Nuclear Moments*, Academic Press, 1958.
- [2] B. Castel, I.S. Towner, *Modern Theories of Nuclear Moments*, Oxford Studies in Nuclear Physics, vol. 12, Clarendon Press, 1990, <https://global.oup.com/academic/product/modern-theories-of-nuclear-moments-9780198517283>.
- [3] G. Neyens, Nuclear magnetic and quadrupole moments for nuclear structure research on exotic nuclei, *Rep. Prog. Phys.* 66 (4) (2003) 633–689, <https://doi.org/10.1088/0034-4885/66/4/205>.
- [4] A.R. Vernon, R.F. Garcia Ruiz, T. Miyagi, C.L. Binnersley, J. Billowes, M.L. Bissell, J. Bonnard, T.E. Cocolios, J. Dobaczewski, G.J. Farooq-Smith, K.T. Flanagan, G. Georgiev, W. Gins, R.P. de Groote, R. Heinke, J.D. Holt, J. Hastings, Á. Koszorus, D. Leimbach, K.M. Lynch, G. Neyens, S.R. Stroberg, S.G. Wilkins, X.F. Yang, D.T. Yordanov, Nuclear moments of indium isotopes reveal abrupt change at magic number 82, *Nature* 607 (2022) 260, <https://doi.org/10.1038/s41586-022-04818-7>.
- [5] N.J. Stone, Table of nuclear magnetic dipole and electric quadrupole moments, *At. Data Nucl. Data Tables* 90 (1) (2005) 75–176, <https://doi.org/10.1016/j.adt.2005.04.001>, <http://www.sciencedirect.com/science/article/pii/S0092640X05000239>.
- [6] N.J. Stone, Table of nuclear magnetic dipole and electric quadrupole moments, report INDC(NDS)-0658, INDC International Nuclear Data Committee, 2014, https://inis.iaea.org/search/search.aspx?orig_q=RN:45029196.
- [7] N.J. Stone, Table of nuclear electric quadrupole moments, *At. Data Nucl. Data Tables* 111–112 (2016) 1–28, <https://doi.org/10.1016/j.adt.2015.12.002>, <http://www.sciencedirect.com/science/article/pii/S0092640X16000024>.
- [8] A.E. Barzakh, D. Atanasov, A.N. Andreyev, M. Al Monthery, N.A. Althubiti, B. Andel, S. Antalic, K. Blaum, T.E. Cocolios, J.G. Cubiss, P. Van Duppen, T.D. Goodacre, A. de Roubin, Y.A. Demidov, G.J. Farooq-Smith, D.V. Fedorov, V.N. Fedosseev, D.A. Fink, L.P. Gaffney, L. Ghys, R.D. Harding, D.T. Joss, F. Herfurth, M. Huysse, N. Imai, M.G. Kozlov, S. Kreim, D. Lunney, K.M. Lynch, V. Manea, B.A. Marsh, Y. Martinez Palenzuela, P.L. Molkanov, D. Neidherr, R.D. Page, M. Rosenbusch, R.E. Rossel, S. Rothe, L. Schweikhard, M.D. Seliverstov, S. Sels, C. Van Beveren, E. Verstraelen, A. Welker, F. Wienholtz, R.N. Wolf, K. Zuber, Hyperfine anomaly in gold and magnetic moments of $I^\pi = 11/2^-$ gold isomers, *Phys. Rev. C* 101 (2020) 034308, <https://doi.org/10.1103/PhysRevC.101.034308>, <https://link.aps.org/doi/10.1103/PhysRevC.101.034308>.
- [9] F. Kondev, M. Wang, W. Huang, S. Naimi, G. Audi, The NUBASE2020 evaluation of nuclear physics properties, *Chin. Phys. C* 45 (3) (2021) 030001, <https://doi.org/10.1088/1674-1137/abddae>.
- [10] W. Huang, M. Wang, F. Kondev, G. Audi, S. Naimi, The AME 2020 atomic mass evaluation (I). Evaluation of input data, and adjustment procedures, *Chin. Phys. C* 45 (3) (2021) 030002, <https://doi.org/10.1088/1674-1137/abddb0>.
- [11] J. Carlson, S. Gandolfi, F. Pederiva, S.C. Pieper, R. Schiavilla, K.E. Schmidt, R.B. Wiringa, Quantum Monte Carlo methods for nuclear physics, *Rev. Mod. Phys.* 87 (2015) 1067–1118, <https://doi.org/10.1103/RevModPhys.87.1067>, <https://link.aps.org/doi/10.1103/RevModPhys.87.1067>.
- [12] J. Henderson, G. Hackman, P. Ruotsalainen, S. Stroberg, K. Launey, J. Holt, F. Ali, N. Bernier, M. Bentley, M. Bowry, R. Caballero-Folch, L. Evitts, R. Frederick, A. Garnsworthy, P. Garrett, B. Jigmeddorj, A. Kilic, J. Lassen, J. Measures, D. Muecher, B. Olaizola, E. O'Sullivan, O. Paetkau, J. Park, J. Smallcombe, C. Svensson, R. Wadsworth, C. Wu, Testing microscopically derived descriptions of nuclear collectivity: Coulomb excitation of ^{22}Mg , *Phys. Lett. B* 782 (2018) 468–473, <https://doi.org/10.1016/j.physletb.2018.05.064>, <https://www.sciencedirect.com/science/article/pii/S0370269318304283>.
- [13] S. Pastore, S.C. Pieper, R. Schiavilla, R.B. Wiringa, Quantum Monte Carlo calculations of electromagnetic moments and transitions in $A \leq 9$ nuclei with meson-exchange currents derived from chiral effective field theory, *Phys. Rev. C* 87 (2013) 035503, <https://doi.org/10.1103/PhysRevC.87.035503>, <https://link.aps.org/doi/10.1103/PhysRevC.87.035503>.
- [14] S.R. Stroberg, J. Henderson, G. Hackman, P. Ruotsalainen, G. Hagen, J.D. Holt, Systematics of $e2$ strength in the sd shell with the valence-space in-medium similarity renormalization group, *Phys. Rev. C* 105 (2022) 034333, <https://doi.org/10.1103/PhysRevC.105.034333>, <https://link.aps.org/doi/10.1103/PhysRevC.105.034333>.
- [15] J. Papuga, M.L. Bissell, K. Kreim, K. Blaum, B.A. Brown, M. De Rydt, R.F. Garcia Ruiz, H. Heylen, M. Kowalska, R. Neugart, G. Neyens, W. Nörtershäuser, T. Otsuka, M.M. Rajabali, R. Sánchez, Y. Utsuno, D.T. Yordanov, Spins and magnetic moments of ^{49}K and ^{51}K : establishing the $1/2^+$ and $3/2^+$ level ordering beyond $N = 28$, *Phys. Rev. Lett.* 110 (2013) 172503, <https://doi.org/10.1103/PhysRevLett.110.172503>, <https://link.aps.org/doi/10.1103/PhysRevLett.110.172503>.
- [16] A. Klose, K. Minamisono, A.J. Miller, B.A. Brown, D. Garand, J.D. Holt, J.D. Lantis, Y. Liu, B. Maaß, W. Nörtershäuser, S.V. Pineda, D.M. Rossi, A. Schwenk, F. Sommer, C. Sumithrarachchi, A. Teigelhöfer, J. Watkins, Ground-state electromagnetic moments of ^{37}Ca , *Phys. Rev. C* 99 (2019) 061301, <https://doi.org/10.1103/PhysRevC.99.061301>, <https://link.aps.org/doi/10.1103/PhysRevC.99.061301>.
- [17] L.V. Rodríguez, D.L. Balabanski, M.L. Bissell, K. Blaum, B. Cheal, G. De Gregorio, J. Ekman, R.F. Garcia Ruiz, A. Gargano, G. Georgiev, W. Gins, C. Gorges, H. Heylen, A. Kanellakopoulos, S. Kaufmann, V. Lagaki, S. Lechner, B. Maaß, S. Malbrunot-Ettenauer, R. Neugart, G. Neyens, W. Nörtershäuser, S. Sailer, R. Sánchez, S. Schmidt, L. Wehner, C. Wraith, L. Xie, Z.Y. Xu, X.F. Yang, D.T. Yordanov, Doubly-magic character of ^{132}Sn studied via electromagnetic moments of ^{133}Sn , *Phys. Rev. C* 102 (2020) 051301, <https://doi.org/10.1103/PhysRevC.102.051301>, <https://link.aps.org/doi/10.1103/PhysRevC.102.051301>.
- [18] B. Sabbey, M. Bender, G.F. Bertsch, P.-H. Heenen, Global study of the spectroscopic properties of the first 2^+ state in even-even nuclei, *Phys. Rev. C* 75 (2007) 044305, <https://doi.org/10.1103/PhysRevC.75.044305>, <https://link.aps.org/doi/10.1103/PhysRevC.75.044305>.
- [19] J.P. Delaroche, M. Girod, J. Libert, H. Goutte, S. Hilaire, S. Péru, N. Pillet, G.F. Bertsch, Structure of even-even nuclei using a mapped collective Hamiltonian and the D1S Gogny interaction, *Phys. Rev. C* 81 (2010) 014303, <https://doi.org/10.1103/PhysRevC.81.014303>, <https://link.aps.org/doi/10.1103/PhysRevC.81.014303>.
- [20] B. Bally, B. Avez, M. Bender, P.-H. Heenen, Beyond mean-field calculations for odd-mass nuclei, *Phys. Rev. Lett.* 113 (2014) 162501, <https://doi.org/10.1103/PhysRevLett.113.162501>, <https://link.aps.org/doi/10.1103/PhysRevLett.113.162501>.
- [21] L. Bonneau, N. Minkov, D.D. Duc, P. Quentin, J. Bartel, Effect of core polarization on magnetic dipole moments in deformed odd-mass nuclei, *Phys. Rev. C* 91 (2015) 054307, <https://doi.org/10.1103/PhysRevC.91.054307>, <https://link.aps.org/doi/10.1103/PhysRevC.91.054307>.
- [22] M. Borrajo, J.L. Egido, Ground-state properties of even and odd magnesium isotopes in a symmetry-conserving approach, *Phys. Lett. B* 764 (2017) 328–334, <https://doi.org/10.1016/j.physletb.2016.11.037>, <http://www.sciencedirect.com/science/article/pii/S0370269316307006>.
- [23] J. Li, J. Meng, Nuclear magnetic moments in covariant density functional theory, *Front. Phys.* 13 (2018) 132109, <https://doi.org/10.1007/s11467-018-0842-7>.
- [24] S. Péru, S. Hilaire, S. Goriely, M. Martini, Description of magnetic moments within the Gogny Hartree-Fock-Bogolyubov framework: application to Hg isotopes, *Phys. Rev. C* 104 (2021) 024328, <https://doi.org/10.1103/PhysRevC.104.024328>, <https://link.aps.org/doi/10.1103/PhysRevC.104.024328>.
- [25] A. Barzakh, A.N. Andreyev, C. Raison, J.G. Cubiss, P. Van Duppen, S. Péru, S. Hilaire, S. Goriely, B. Andel, S. Antalic, M. Al Monthery, J.C. Berengut, J. Bieroń, M.L. Bissell, A. Borschevsky, K. Chrysalidis, T.E. Cocolios, T. Day Goodacre, J.-P. Dognon, M. Elantkowska, E. Eliav, G.J. Farooq-Smith, D.V. Fedorov, V.N. Fedosseev, L.P. Gaffney, R.F. Garcia Ruiz, M. Godefroid, C. Granados, R.D. Harding, R. Heinke, M. Huysse, J. Karls, P. Marmonier, J.G. Li, K.M. Lynch, D.E. Maison, B.A. Marsh, P. Molkanov, P. Mosat, A.V. Olenichenko, V. Panteleev, P. Pyykkö, M.L. Reitsma, K. Rezykina, R.E. Rossel, S. Rothe, J. Ruczkowski, S. Schiffmann, C. Seiffert, M.D. Seliverstov, S. Sels, L.V. Skripnikov, M. Stryczek, D. Studer, M. Verlinde, S. Wilman, A.V. Zaitsevskii, Large shape staggering in neutron-deficient Bi isotopes, *Phys. Rev. Lett.* 127 (2021) 192501, <https://doi.org/10.1103/PhysRevLett.127.192501>, <https://link.aps.org/doi/10.1103/PhysRevLett.127.192501>.
- [26] W. Ryssens, G. Scamps, S. Goriely, M. Bender, Skyrme-Hartree-Fock-Bogolyubov mass models on a 3D mesh: II. Time-reversal symmetry breaking, *Eur. Phys. J. A* 58 (2022) 246, <https://doi.org/10.1140/epja/s10050-022-00894-5>.
- [27] B. Bally, G. Giacalone, M. Bender, Structure of $^{128,129,130}\text{Xe}$ through multi-reference energy density functional calculations, *Eur. Phys. J. A* 58 (2022) 187, <https://doi.org/10.1140/epja/s10050-022-00833-4>.
- [28] P.L. Sassarini, J. Dobaczewski, J. Bonnard, R.F. Garcia Ruiz, Nuclear DFT analysis of electromagnetic moments in odd near doubly magic nuclei, *J. Phys. G, Nucl. Part. Phys.* 49 (11) (2022) 11LT01, <https://doi.org/10.1088/1361-6471/ac900a>.
- [29] G.F. Bertsch, L.M. Robledo, Symmetry restoration in Hartree-Fock-Bogolyubov based theories, *Phys. Rev. Lett.* 108 (2012) 042505, <https://doi.org/10.1103/PhysRevLett.108.042505>, <https://link.aps.org/doi/10.1103/PhysRevLett.108.042505>.
- [30] B. Avez, M. Bender, Evaluation of overlaps between arbitrary fermionic quasiparticle vacua, *Phys. Rev. C* 85 (2012) 034325, <https://doi.org/10.1103/PhysRevC.85.034325>, <https://link.aps.org/doi/10.1103/PhysRevC.85.034325>.
- [31] J. Dobaczewski, J. Dudek, Solution of the Skyrme-Hartree-Fock equations in the Cartesian deformed harmonic-oscillator basis. (III) hfodd (v1.75r): a new version of the program, *Comput. Phys. Commun.* 131 (1) (2000) 164–186, [https://doi.org/10.1016/S0010-4655\(00\)00121-1](https://doi.org/10.1016/S0010-4655(00)00121-1), <http://www.sciencedirect.com/science/article/pii/S0010465500001211>.
- [32] J. Dobaczewski, W. Satuła, B. Carlsson, J. Engel, P. Olbratowski, P. Powalowski, M. Sadziak, J. Sarich, N. Schunck, A. Staszczak, M. Stoitsov, M. Zalewski, H. Zduneczuk, Solution of the Skyrme-Hartree-Fock-Bogolyubov equations in the Cartesian deformed harmonic-oscillator basis. (VI) hfodd

- (v2.40h): a new version of the program, *Comput. Phys. Commun.* 180 (11) (2009) 2361–2391, <https://doi.org/10.1016/j.cpc.2009.08.009>, <http://www.sciencedirect.com/science/article/pii/S0010465509002598>.
- [33] G. Bertsch, J. Dobaczewski, W. Nazarewicz, J. Pei, Hartree-Fock-Bogoliubov theory of polarized Fermi systems, *Phys. Rev. A* 79 (2009) 043602, <https://doi.org/10.1103/PhysRevA.79.043602>, <https://link.aps.org/doi/10.1103/PhysRevA.79.043602>.
- [34] J. Dobaczewski, P. Olbratowski, Solution of the Skyrme-Hartree-Fock-Bogoliubov equations in the Cartesian deformed harmonic-oscillator basis. (IV) hfodd (v2.08i): a new version of the program, *Comput. Phys. Commun.* 158 (3) (2004) 158–191, <https://doi.org/10.1016/j.cpc.2004.02.003>, <http://www.sciencedirect.com/science/article/pii/S0010465504000797>.
- [35] J. Dobaczewski, P. Bączyk, P. Becker, M. Bender, K. Bennaceur, J. Bonnard, Y. Gao, A. Idini, M. Koniczka, M. Kortelainen, L. Próchniak, A.M. Romero, W. Satuła, Y. Shi, L.F. Yu, T.R. Werner, Solution of universal nonrelativistic nuclear DFT equations in the Cartesian deformed harmonic-oscillator basis, in: (IX) HFODD (v3.06h): A New Version of the Program, *J. Phys. G, Nucl. Part. Phys.* 48 (10) (2021) 102001, <https://doi.org/10.1088/1361-6471/ac0a82>.
- [36] J. Dobaczewski, et al., *J. Phys. G, Nucl. Part. Phys.* (2023), in preparation.
- [37] Version (v3.16n) of code hfodd that was used in this study along with the corresponding raw input and output data files are available in the data repository at <https://webfiles.york.ac.uk/HFODD/Projects/GadLead>.
- [38] P. Ring, P. Schuck, *The Nuclear Many-Body Problem*, Springer-Verlag, Berlin, 1980, <https://www.springer.com/gp/book/9783540212065>.
- [39] J.A. Sheikh, J. Dobaczewski, P. Ring, L.M. Robledo, C. Yannouleas, Symmetry restoration in mean-field approaches, *J. Phys. G, Nucl. Part. Phys.* 48 (12) (2021) 123001, <https://doi.org/10.1088/1361-6471/ac288a>.
- [40] L.M. Robledo, Sign of the overlap of Hartree-Fock-Bogoliubov wave functions, *Phys. Rev. C* 79 (2009) 021302, <https://doi.org/10.1103/PhysRevC.79.021302>, <http://link.aps.org/doi/10.1103/PhysRevC.79.021302>.
- [41] Supplemental Material at [URL will be inserted by publisher], which includes Refs. [51–61], presents precision tests of the particle-number projection and intrinsic quadrupole moments, give details of the Bayesian model averaging (BMA) analysis, and present precision tests related to using the Harmonic-oscillator basis. There we also tabulate the numerical values pertaining to the results discussed in the body of the paper, and show plots of the potential energy surfaces.
- [42] M. Kortelainen, J. McDonnell, W. Nazarewicz, P.-G. Reinhard, J. Sarich, N. Schunck, M.V. Stoitsov, S.M. Wild, Nuclear energy density optimization: large deformations, *Phys. Rev. C* 85 (2012) 024304, <https://doi.org/10.1103/PhysRevC.85.024304>, <https://link.aps.org/doi/10.1103/PhysRevC.85.024304>.
- [43] G. Gall, B. Bonche, J. Dobaczewski, H. Flocard, P.-H. Heenen, Superdeformed rotational bands in the mercury region. A cranked Skyrme-Hartree-Fock-Bogoliubov study, *Z. Phys. A* 348 (1994) 183, <https://doi.org/10.1007/BF01291916>.
- [44] N. Schunck, J. Dobaczewski, J. McDonnell, W. Satuła, J. Sheikh, A. Staszczak, M. Stoitsov, P. Toivanen, Solution of the Skyrme-Hartree-Fock-Bogoliubov equations in the Cartesian deformed harmonic-oscillator basis: (VII) hfodd (v2.49t): a new version of the program, *Comput. Phys. Commun.* 183 (1) (2012) 166–192, <https://doi.org/10.1016/j.cpc.2011.08.013>, <http://www.sciencedirect.com/science/article/pii/S0010465511002852>.
- [45] T. Schmidt, Über die magnetischen Momente der Atomkerne, *Z. Phys.* 106 (1937) 358–361, <https://doi.org/10.1007/BF01338744>.
- [46] O. Häusser, P. Taras, W. Trautmann, D. Ward, T.K. Alexander, H.R. Andrews, B. Haas, D. Horn, g factors of high-spin yrast traps in $^{146,147}\text{Gd}$, *Phys. Rev. Lett.* 42 (1979) 1451–1454, <https://doi.org/10.1103/PhysRevLett.42.1451>, <https://link.aps.org/doi/10.1103/PhysRevLett.42.1451>.
- [47] O. Häusser, H.E. Mahnke, T.K. Alexander, H.R. Andrews, J.F. Sharpey-Schafer, M.L. Swanson, D. Ward, P. Taras, J. Keinonen, Quadrupole moments of yrast isomers in $^{144,147,148}\text{Gd}$, *Nucl. Phys. A* 379 (2) (1982) 287–312, [https://doi.org/10.1016/0375-9474\(82\)90394-3](https://doi.org/10.1016/0375-9474(82)90394-3), <https://www.sciencedirect.com/science/article/pii/0375947482903943>.
- [48] E. Dafni, J. Bendahan, C. Broude, G. Goldring, M. Hass, E. Lahmer-Naim, M.H. Rafailovich, N. Ayres De Campos, A. Gelberg, g-factors of short-lived isomers in $^{147,148}\text{Gd}$ and the role of the 3^- core excitation, *Phys. Lett. B* 199 (1) (1987) 26–29, [https://doi.org/10.1016/0370-2693\(87\)91457-2](https://doi.org/10.1016/0370-2693(87)91457-2), <https://www.sciencedirect.com/science/article/pii/0370269387914572>.
- [49] J. Bonnard et al., 2023 in preparation.
- [50] A. Bohr, B.R. Mottelson, *Nuclear Structure*, vol. II, W. A. Benjamin, Reading, 1975, §4-3c.
- [51] H. Wibowo, et al., *J. Phys. G, Nucl. Part. Phys.* (2023), in preparation.
- [52] D. Varshalovich, A. Moskalev, V. Khersonskii, *Quantum Theory of Angular Momentum*, World Scientific, Singapore, 1988.
- [53] E. Chabanat, P. Bonche, P. Haensel, J. Meyer, R. Schaeffer, A Skyrme parametrization from subnuclear to neutron star densities Part II. Nuclei far from stabilities, *Nucl. Phys. A* 635 (1) (1998) 231.
- [54] P.-G. Reinhard, Skyrme forces and giant resonances in exotic nuclei, *Nucl. Phys. A* 649 (1999) 305c, [https://doi.org/10.1016/S0375-9474\(99\)00076-7](https://doi.org/10.1016/S0375-9474(99)00076-7).
- [55] J. Dobaczewski, W. Nazarewicz, P. Reinhard, Error estimates of theoretical models: a guide, *J. Phys. G, Nucl. Part. Phys.* 41 (7) (2014) 074001, <http://stacks.iop.org/0954-3889/41/i=7/a=074001>.
- [56] D. Sivia, *Data Analysis: A Bayesian Tutorial*, Clarendon Press, 1996.
- [57] B.D. Carlsson, A. Ekström, C. Forssén, D.F. Strömberg, G.R. Jansen, O. Lilja, M. Lindby, B.A. Mattsson, K.A. Wendt, Uncertainty analysis and order-by-order optimization of chiral nuclear interactions, *Phys. Rev. X* 6 (2016) 011019, <https://doi.org/10.1103/PhysRevX.6.011019>, <https://link.aps.org/doi/10.1103/PhysRevX.6.011019>.
- [58] M. Bender, J. Dobaczewski, J. Engel, W. Nazarewicz, Gamow-Teller strength and the spin-isospin coupling constants of the Skyrme energy functional, *Phys. Rev. C* 65 (2002) 054322, <https://doi.org/10.1103/PhysRevC.65.054322>, <http://link.aps.org/doi/10.1103/PhysRevC.65.054322>.
- [59] J.A. Hoeting, D. Madigan, A.E. Raftery, C.T. Volinsky, Bayesian model averaging: a tutorial (with comments by M. Clyde, David Draper and E.I. George, and a rejoinder by the authors, *Stat. Sci.* 14 (4) (1999) 382–417, <https://doi.org/10.1214/ss/1009212519>.
- [60] J. Dobaczewski, J. Dudek, Solution of the Skyrme-Hartree-Fock equations in the Cartesian deformed harmonic oscillator basis II. The program hfodd, *Comput. Phys. Commun.* 102 (1) (1997) 183–209, [https://doi.org/10.1016/S0010-4655\(97\)00005-2](https://doi.org/10.1016/S0010-4655(97)00005-2), <http://www.sciencedirect.com/science/article/pii/S0010465597000052>.
- [61] M. Kortelainen, 2023, in preparation.